Preliminary JIRAM Results From Juno Polar Observations: 2 - Analysis of the Jupiter Southern H_3^+ emissions and Comparison with the North Aurora

A. Adriani[1], A. Mura[1], M.L. Moriconi[2], B.M. Dinelli[2], F. Fabiano[2,3], F. Altieri[1], G. Sindoni[1], G. Filacchione[1], F. Tosi[1], A. Migliorini[1], D. Grassi[1], G. Piccioni[1], R. Noschese[1], A. Cicchetti[1], S.J. Bolton[4], J.E.P. Connerney[5], S.K. Atreya[6], F. Bagenal[7], G.R. Gladstone[4], C. Hansen[8], W.S. Kurth[9], S.M. Levin[10], J.I. Lunine[11], B.H. Mauk[12], D.J. McComas[13], D. Turrini[1], S. Stefani[1], and M. Amoroso[14]

[1]INAF-Istituto di Astrofisica e Planetologia Spaziali, Roma, Italy
[2]CNR-Istituto di Scienze dell'Atmosfera e del Clima, Bologna e Roma, Italy
[3]Dipartimento di Fisica e Astronomia, Università di Bologna
[4]Southwest Research Institute, San Antonio, Texas, USA
[5]NASA Goddard Space Flight Center, Greenbelt, Maryland, USA
[6]University of Michigan, Ann Arbor, Michigan, USA
[7]University of Colorado, Boulder, Colorado, USA
[8]Planetary Science Institute, Tucson, Arizona, USA
[9]Jet Propulsion Laboratory, California Institute of Technology, Pasadena, California, USA
[10]University of Iowa, Iowa City, Iowa, USA
[11]Cornell University, Ithaca, New York, USA
[12]The Johns Hopkins University Applied Physics Laboratory, Laurel, Maryland, USA
[13]PPPL, Princeton University, New Jersey, USA
[14]Agenzia Spaziale Italiana, Roma, Italy

Corresponding author: Alberto Adriani (alberto.adriani@iaps.inaf.it)

Key Points:

- H_3^+ intensity, column density and temperature maps on the Jupiter Southern aurora from Juno/JIRAM spectrometer data from first orbit data
- Emissions from Southern aurora are more intense than the Northern ones.

Abstract

The Jupiter Auroral InfraRed Mapper (JIRAM) aboard Juno observed the Jovian South Pole Aurora during the first orbit of the mission. H_3^+ (trihydrogen cation) and CH_4 (methane) emissions have been identified and measured. The observations have been carried out in nadir and slant viewing both by the L-filtered imager and the spectrometer. The coverage of the main oval during these perijove measurements has been partial, but sufficient to determine different regions of temperature and abundance of the H_3^+ ion from its emission lines in the 3-4 μm wavelength range. Abundances of the CH_4 too have also been derived from the 3.3 μm line emission underlying the H_3^+ spectrum.

1 Introduction

The Juno mission [*Bolton et al*, 2017 and *Connerney et al*, 2017] gives to the scientific community the first occasion to study the South Pole aurora of Jupiter in homogeneous and simultaneous observing conditions. Past analyses (*Kim et al.*, 2015 and 2009; *Giles et al*, 2016), carried out from ground-based observations, underwent and tried to solve some difficulties in spectral matching due to different dates and sky conditions of the datasets. The Juno mission has among its primary objectives indeed the auroral mechanisms' exploitation and its polar orbital planning gives to JIRAM many opportunities to target and detect emissions and morphology of the auroral features over and over from different distances and with a variety of viewing angles. JIRAM is essentially composed by a spectrometer and an imager, sharing the same telescope [*Adriani et al*., 2014, 2016]. The imager focal plane is, in turn, divided in two equal areas defined by the superimposition of two different band-pass filters: an L-filter, centered at 3.45 μm with a 290 nm bandwidth, and an M-filter, centered at 4.78 μm with a 480 nm bandwidth. The spectrometer's slit is co-located in the M-filter imager's FOV and its spectral range covers the 2-5 μm interval in 336 spectral bins (bands). The instrument design allows the imaging of the auroral features both spatially and spectrally in a unique session. Custom planning of the spectrometer measurements has been also set in the perspective to match consecutive acquisitions to obtain a quite simultaneous spectral image. While the spacecraft is spinning in order to keep its attitude by inertia against radiation disturbances on the navigation system, JIRAM is equipped by a despinning mirror that permits to keep the target image still in the field of view during the data acquisition [*Adriani et al.*, 2014]. The de-spinning mirror has also the possibility to be activated at different times in respect to the nadir direction, by using data about the spacecraft dynamics, allowing a scanning of the planet in the spacecraft's spinning plane. No pointing outside of the spinning plane is permitted.

JIRAM spectral observation have been used in the present work to give spatially detailed analysis of H_3^+ temperatures and column densities of the South Pole Aurora, assuming a quasi-local thermal equilibrium for H_3^+ [*Stallard et al*, 2002], whose results are summarized in a series of maps. In section 2 we mention the observation strategies and data management and mapping are given along with the method applied to retrieve effective temperatures and column densities of the emitting molecules along the line of sight. Other specific auroral topics like morphology and dynamics are described by Mura et al. (this issue). In Section 3 the preliminary results will be discussed and compared with the findings reported in the previous literature.

2 Observations and Data Management

The first JIRAM observations on the Southern aurora were acquired on 27 August 2016, in the outbound leg of the first orbit, from 15:00 to 19:45 UTC. During that period, the spacecraft was moving away from the planet and the instrument had Jupiter's southern hemisphere in its field of view. The spatial resolution at the 1-bar level ranged between 45 and 135 km. The spectrometer's slits mosaic reported in Figure 1 gives the complete survey of the spectral

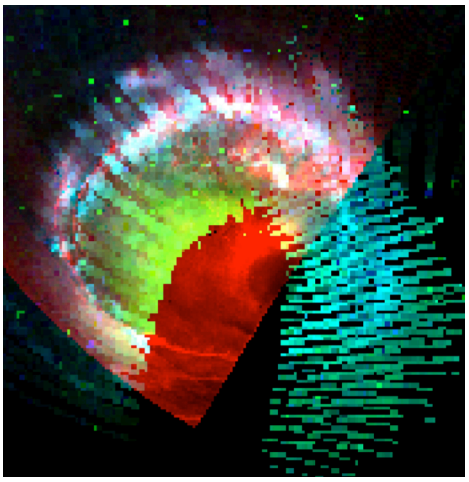

Figure 1. RGB spectrometer-imager composition of the southern aurora. The Red comes from an imager acquisition of the aurora (4.54-5.02 μm). Green is set at 3.3149 μm where the H_3^+ emission is overlaid to the CH_4 Q branch, and Blue is set at 3.5397 μm a H_3^+ emission band.

observations of the Southern aurora. The spectral mosaic is superimposed to a single L-band image taken by the JIRAM imager for context reference. Figure 1 has been mapped in a polar stereographic projection. The two kind of acquisitions have been first of all geo-located to a common reference ellipse and datum, then re-projected in Sys III planetocentric geographical coordinates. Geometric information was obtained by using ad hoc algorithms based on the NAIF-SPICE tool [*Acton*, 1996] and radiometrically calibrated in units of spectral radiance (W/m^2 μm sr) according to *Adriani et al.* [2014]. It should be noted that the L-band side of the imager and the spectrometer's slit do not simultaneously observe the same scene, even if they are operated at the same time as the spectrometer slit is optically combined with the M-band side of the imager dedicated to the thermal emission of the planet. The L-band imager covers a Field of View (FOV) of about 1.75° by 6° while the spectrometer's slit is sampled in 256 spatial pixels, each with an individual field of view of about 240 μrad for a total coverage of about 3.5° (see Adriani et al., 2104, for instrumental details). However the spectrometer slit can scan the same area of the L-band imager in times subsequent to the imager acquisition. Figure 1 is a RGB color composition of the southern aurora observed during PJ1, where the mosaic from the imager has been set in red while the green and the blue correspond to two different spectrometer channels selected among the H_3^+ emission line wavelengths: the green corresponds to the 3.3149 μm wavelength, where the H_3^+ emission is overlaid to the CH_4 Q branch, and indicates wherever this

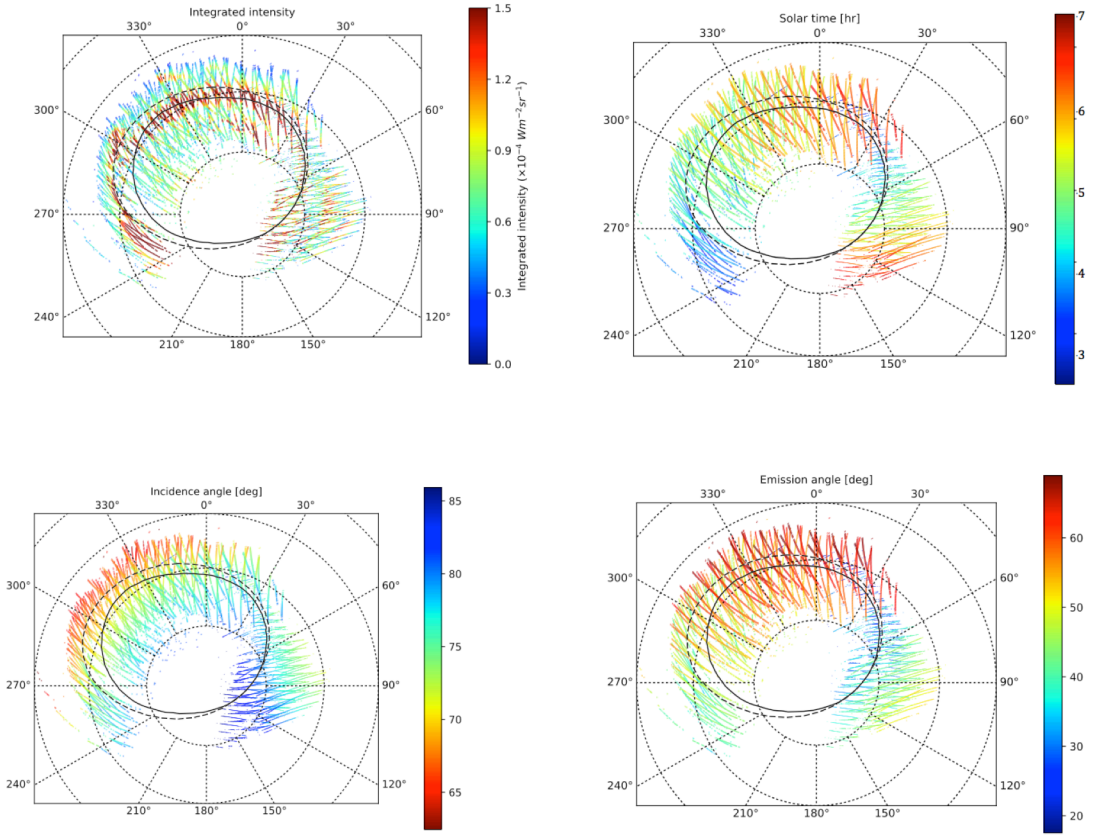

Figure 2. Southern aurora observational parameters: H_3^+ auroral emissions integrated in the range 3.35 to 3.75 μm (upper left); Time of the Jovian day upper right); Solar Zenith Angle (SZA) (lower left); and Emission Zenith Angle (angular direction of the spacecraft in respect the emitting area) (lower right). Latitudes are spaced by 10 degrees. The continuous curve oval is from VIP4 model [*Connerney et al.*, 1998]; the dashed curve oval it the statistical one from ground-based observations [*Bagenal et al.*, 2014].

hydrocarbon is present and emitting; the blue is set at 3.5397 μm, where the infrared aurora has one of its stronger emission bands. This rendering emphasizes the coincidence of the main oval features between spectrometer and imager. Indeed the auroral shape appears white where the two images overlap, attesting that the green and blue spectral traces spatially converge on the red imager one. The size of the pixels on the figure is just proportional to the actual spatial dimension of the instrument pixels' FOV. The drifting of the image color from white to green in the inner part of auroral oval suggests a non-negligible presence of methane being the 3.3149 μm band amplitude significantly higher than expected for H_3^+ compared to the other emission bands. The analysis and the relative discussion about the presence of methane auroral emissions have been analyzed in separate paper by *Moriconi et al.* (this issue).

3 Analysis and Discussion

Figure 2 reports the observational parameters for the southern hemisphere in those areas where the spectrometer was able to scan the planet. Here each spatial pixel is plotted on a stereographic map referred to a surface at 500 km above the usual 1-bar reference level used for Jupiter. The 500-km surface is expected the be closer to the real position of the maximum of the active H_3^+, therefore providing a better match of the auroral features with respect to the underlying planet for slant observations. The radiances corresponding to the H_3^+ emission band between 3.35 and 3.75 μm have been integrated to highlight the position of the H_3^+ aurora and keep out of the contribution to the emission from methane at 3.32 μm. The integrated radiances have been multiplied by the cosine of the emission angle, to correct for the observational slant optical path. The dashed curve gives the position of the auroral oval according to the expected location based on the statistics from the ground-based observations of the southern aurora [*Bagenal et al.*, 2014] and the continuous curve account for the predicted position by the VIP4 model [*Connerney et al.*, 1998]. In the period of acquisition the planet rotated for about 180° so that we cannot address any specific Sun direction in the maps of the figure. Then, beside the integrated radiance, Figure 2 gives also other information about the observations like the Jupiter time of the day due to the solar position in respect of the observational attitude, the solar zenith angle (SZA) and the emission angle. All the observations of the southern aurora have been taken on the Jovian dayside and no measurements are available for the nocturnal time.

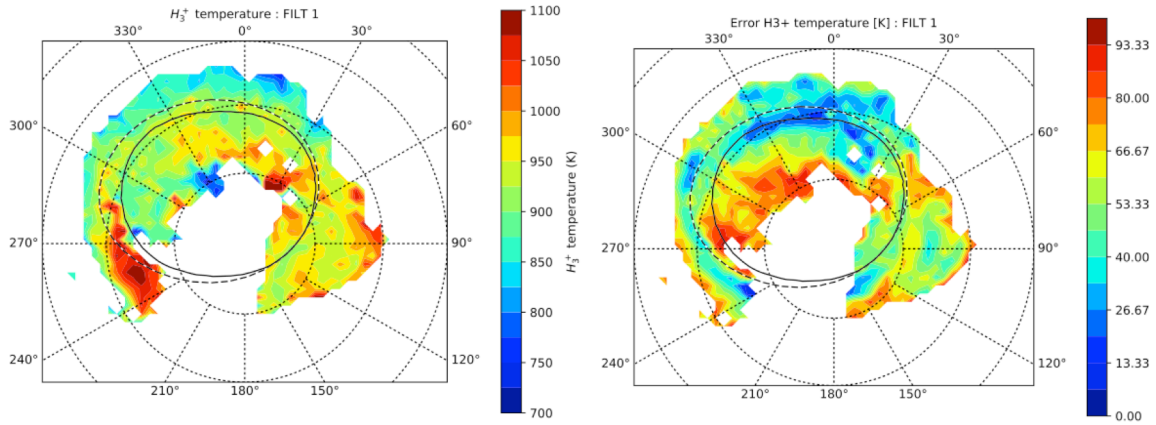

Figure 3. H_3^+ effective temperature (left panel) and error on its retrieval (right panel). The continuous curve oval is from VIP4 model [Connerney et al., 1998]; the dashed curve oval it the statistical one from ground-based observations [Bagenal et al., 2014]. Latitudes are spaced by 10 degrees.

The absolute and relative intensities of the H_3^+ emission bands are directly related respectively to the number of emitting ions and their effective temperatures, so H_3^+ column densities and temperatures have been computed according to the method applied by Dinelli et al. (this issue) to the northern hemisphere auroral data. Then a characterization of the southern aurora has been carried out by computing the H_3^+ effective temperatures and the column densities at the different location where the infrared auroral emissions are present. Only spectra with an emission angle smaller than 75° have been retained in the analysis and the results of the analysis were further

filtered by retaining only the retrievals of the spectra for which the final χ^2 test was smaller than 20, and the retrieved T had a formal error smaller than 100 K. No filter was applied to the size of the error on the H_3^+ column densities. Figure 3 shows the H_3^+ temperature field, which values range between 900K and 1100K. The orthographic surface shown in the panels of Figure 3, and the following Figure 4, has been divided into squared bins, obtained by dividing each axis in regular intervals. The individual intensities have been averaged over each bin, and bins containing less than 3 measurements have been discarded. Figures 3 and 4 represent the contour plot of the binned distribution. In general, the temperature field of the aurora looks quite patchy with the tendency to increase inside the oval. The error on the retrieved temperatures is always below 10% but the presence of methane in the auroral scene impacts the H_3^+ temperature retrieval to some extent. In fact the highest values of the error are obtained where methane emissions exist (see Figure 1). The highest temperature along the oval can be found during the Jovian morning - as can be seen by comparing the temperature maps in Figure 3 and local solar time during the observations in Figure 2- where it reaches values as high as 1100K.
The H_3^+ column density is mapped in Figure 4. The values range in the interval 1-3.5x10^{12} ions/cm^{-2}. After the retrieval the H_3^+ column has been corrected by the emission angle so that values in Figure 4 represent the equivalent vertical column above the 1-bar pressure level. The distribution of the auroral emission is directly proportional to the number of emitting H_3^+ ions, therefore the distribution of the integrated radiance shown in Figure 2 follows the distribution column density reported in Figure 4. The relative error on the retrieved values is lower than 10% in correspondence of the higher column densities and it is maximum in correspondence of the presence of methane.

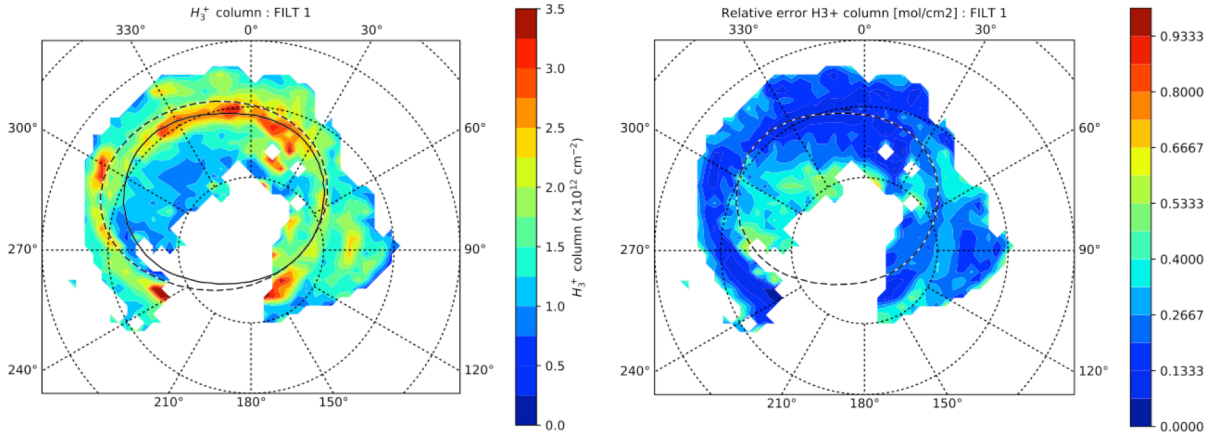

Figure 4. H_3^+ column density (left panel) and error on its retrieval (right panel)**.** The continuous curve oval is from VIP4 model [*Connerney et al*., 1998]; the dashed curve oval it the statistical one from ground-based observations [*Bagenal et al*., 2014]. Latitudes are spaced by 10 degrees

As previously mentioned the observations of the southern aurora have been collected only during daytime while northern observations cover the full Jupiter day of about 10 hours. A comparison between the southern and northern auroral emissions [*Dinelli et al.*, this issue] is given in Figure

5 and the comparison is shown for the period of the day in which both southern and northern data are both available, namely from about 3 h to 7 h local solar time. Figure 5 shows different panels that account for various auroral parameters like the 3.35-3.75 μm integrated radiance and H_3^+ effective temperature as a function of the solar time on the left column. The right column, instead, reports correlations between the same parameters. In the left column the curves have been obtained by a running average on the single parameter values for a points number of points corresponding to about a 1 h time interval, while in the right column the scatter plots of different pairs of retrieved parameters are reported. A North/South direct comparison shows that the integrated radiances display systematic differences. Southern hemisphere auroral emissions appear generally to be always more powerful than the northern ones. In the southern hemisphere the average integrated radiance was (0.89±046)·10-4 W/m^2/sr with the highest values reaching 7.34·10-4 W/m^2/sr while in the North no values greater than 3.38·10-4 W/m^2/sr have been found with a mean value of $(0.75\pm0.34)\cdot10^{-4}$ W/m^2/sr [Dinelli et al., this issue]. Meanwhile the integrated radiances are proportional to the column densities, as expected, the temperature behavior shows different behaviors, namely temperatures tend to be higher for lower column densities. A limited number of regions can reach temperatures as high as 1400K when the column density is about $0.5\cdot10^{12}$ molecules/cm^2 while at the highest column densities the temperatures stay around 900K, on the other hand, temperatures as high as 900 K are recorded in correspondence of the highest column densities values. Unfortunately, the comparison between South and North is not straightforward in respect to their trends versus the time of the day. In fact, it has to be said that the number of observations from the North is limited and not widely distributed over the space when considering the time of the day when South and North are comparable. The Northern auroral observations during the central part of the day come mostly from regions inside the oval (see Dinelli et al., this issue) thus the low values have to be mostly attributed to the location of the auroral emissions. On the other hand the observations taken in the first part of the morning and in the afternoon come from the oval regions. Differently from the North a better information about the diurnal trend of the intensity of the emissions can be read in the Southern data that show an increased intensity of emissions after dawn and before dusk. In order to verify this behavior three independent longitudinal intervals have been selected. In those longitudinal interval observations have been taken during different time of the day (see the lower left panel of Figure 5). The all three areas show the same behavior of the emissions during the day, namely a decrease of the emission during the central part of the day and higher values closer to dawn and dusk. In general, the highest temperatures in the southern hemisphere look to be reached in the first part of the morning, while the staying approximately constant during the rest of the day. At North, also the temperatures show a significant falling in the values around the central part of the day due to the fact that those measurements come mostly from the inner part of the oval.

4 Concluding Remarks

The spatial distribution of temperatures and column densities of the H_3^+ ions responsible for the southern auroral emissions have been analysed in detail for the first time based on Juno/JIRAM data. In some of our maps, the auroral shape has been also compared with the VIP4 model [*Connerney et al*., 1998], which predicts the position of the aurora and according to the statistical model reported in *Bagenal et al.* [2014], giving the average spatial position calculated from many years of ground-based observations. The auroral oval, obtained with the JIRAM L-band images, seems to be in a pretty good agreement with the statistical model, rather than the VIP4

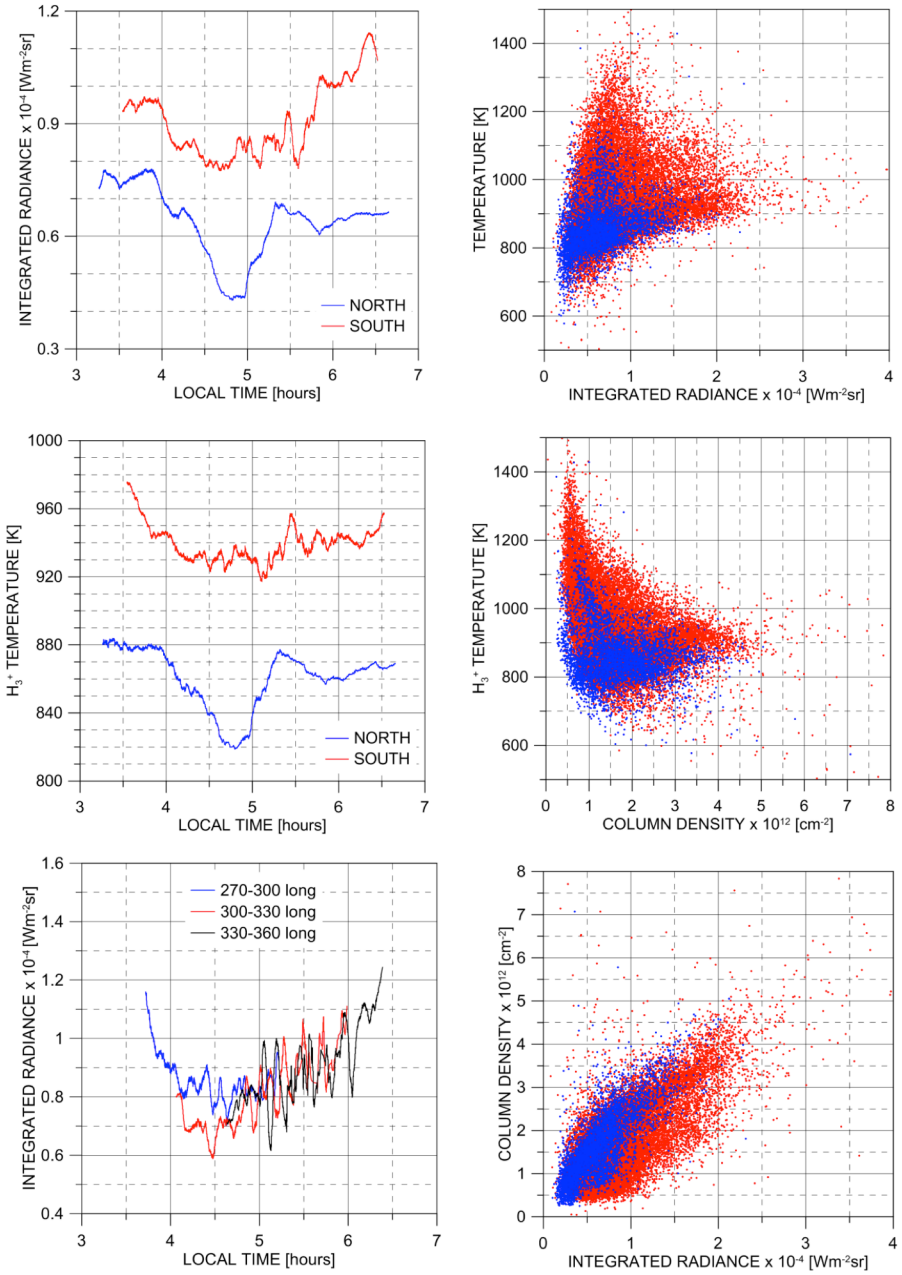

Figure 5. H_3^+ integrated radiance (emissions in the range 3.35 and 3.75 μm) versus the Jovian time of the day (upper left panel), H_3^+ effective temperature versus the Jovian time of the day (central left panel), H_3^+ column density versus the Jovian time of the day (lower left panel), correlations between temperature and integrated radiance (upper right panel), temperature and column density (central right panel), and column density and integrated radiance (lower right panel).

one. The retrieved temperature can vary between 600K and 1400K during the Jovian day with prevalence of higher values in the morning. A comparison of the southern auroral and northern auroral regions show significant differences with the northern aurora both in magnitude and in behavior.

Acknowledgments

The JIRAM project is founded by the Italian Space Agency (ASI). In particular this work has been developed under the agreement n. 2016-23-H.0.

References

Acton, C.H., (1996). Ancillary data services of NASA's navigation and ancillary information facility. Planet. Space. Sci. 44 (1), 65-70

Adriani A., G. Filacchione, T. Di Iorio, D. Turrini, R. Noschese, A. Cicchetti, D. Grassi, A. Mura, G. Sindoni, M. Zambelli, G. Piccioni, M.T. Capria, F. Tosi, R. Orosei, B.M. Dinelli, M.L. Moriconi, E. Roncon, J.I. Lunine, H.N. Becker, A. Bini, A. Barbis, L. Calamai, C. Pasqui, S. Nencioni, M. Rossi, M. Lastri, R. Formaro, A. Olivieri (2014), JIRAM, the Jovian Infrared Auroral Mapper. Space Sci. Rev., DOI 10.1007/s11214-014-0094-y.

Adriani A. , M.L. Moriconi, A. Mura, F.Tosi, G. Sindoni, R. Noschese, A. Cicchetti, G. Filacchione, (2016), Juno's Earth flyby: the Jovian infrared Auroral Mapper preliminary results, Astrophys Space Sci, DOI 10.1007/s10509-016-2842-9

Bagenal F.,A. Adriani, F. Allegrini, S.J. Bolton, B. Bonfond, E.J. Bunce, J.E.P. Connerney, S.W.H. Cowley, R.W. Ebert, G.R. Gladstone, C.J. Hansen, W.S. Kurth, S.M. Levin, B.H. Mauk, D.J. McComas, C.P. Paranicas, D. Santos-Costa, R.M. Thorne, P. Valek, J.H. Waite, P. Zarka (2014), Magnetospheric Science Objectives of the Juno Mission, Space Sci Rev, DOI 10.1007/s11214-014-0036-8.

Bolton S.J., A. Adriani, V. Adumitroaie, J. Anderson, S. Atreya, J. Bloxham, S. Brown, J. E.P. Connerney, E. DeJong, W. Folkner, D. Gautier, S. Gulkis, T. Guillot, C. Hansen,W.B. Hubbard, L. Iess, A. Ingersoll, M. Janssen, J. Jorgensen, Y. Kaspi, S. M. Levin, C. Li, J. Lunine, Y. Miguel, G. Orton, T. Owen, M. Ravine, E. Smith, P. Steffes, E. Stone, D. Stevenson, R. Thorne, J. Waite, (2017), in print on Science

Connerney, J. E. P., M. H. Acuña, N. F. Ness, and T. Satoh (1998) New models of Jupiter's magnetic field constrained by the Io flux tube footprint, J. Geophys. Res., 103(A6), 11,929–11,939.

Connerney J. E.P., A. Adriani, F. Bagenal, J. Bloxham, S. J. Bolton, S. Cowley, J-C. Gerard8, G.R. Gladstone, D. Grodent, G. Hospodarsky, J. Jorgensen, W. Kurth, S. M. Levin, B. Mauk, D. McComas, A. Mura, C. Paranicas, (2017), in print on Science

Dinelli et al., this issue.

Dinelli et Al., this issue.

Giles R.S., L.N. Fletcher, P.G.J. Irwin, H. Melin, and T.S. Stallard (2016), Detection of H+

3 auroral emission in Jupiter's 5-micron window, A&A 589, A67 (2016), DOI: 10.1051/0004-6361/201628170

Kim, S. J., C.K. Sim, J. Ho, T.R. Geballe , Y.L. Yung, S. Miller, Y.H. Kim (2015). Hot CH4 in the polar regions of Jupiter, Icarus, 257, 217–220.

Kim, S. J, T.R. Geballe , H.J. Seo, Y.H. Kim, (2009). Jupiters's hydrocarbon polar brightening: Discovery of 3-micron line emission from south polar CH4, C2H2, and C2H6, Icarus, 202, 354–357.

Moriconi et al., this issue.

Mura et al., this issue.

Stallard T., S. Miller, G. Millward, R.D. Joseph, 2002. On the Dynamics of the Jovian Ionosphere and Thermosphere. II The Measurement of H+3 Vibrational Temperature, Column Density, and Total Emission, Icarus, 156, 498–514.